Model-in-the-Loop Validation of Future-Aware Tertiary Control Layer for CMR Microgrid

Md Jamal Ahmed Shohan[1], *Member, IEEE*, Renuka Loka[1], *Member, IEEE*, Rakesh Shamrao Patekar[1], Mohanad Elsayed[1], Mahmoud Kabalan[*,1], *Senior Member, IEEE*, Mohamed M. Zakaria Moustafa[1], *Member, IEEE*, Thomas Bozada[2]
[1]*Center for Microgrid Research, University of St. Thomas*, Saint Paul, MN, USA
[2]*U.S. Army Engineer Research and Development Center*, Champaign, IL, USA
*Email: mahmoud.kabalan@stthomas.edu

***Abstract*—This paper presents a model-in-the-loop (MIL) validation framework for integrating and testing a future-aware tertiary control layer for the Center for Microgrid Research (CMR) Microgrid. The framework enables closed-loop interaction among forecasting, optimization, and real-time digital simulation, providing a realistic and low-risk environment for evaluating control performance before field deployment. A long short-term memory (LSTM) model is developed for short-term load and photovoltaic (PV) forecasting using real CMR Microgrid data and incorporated into the tertiary control algorithm for future-informed decision-making. The tertiary control layer is integrated with a real-time digital model of the microgrid to allow bidirectional data exchange and execution of control commands based on real-time system feedback. The proposed framework is validated under various operating conditions, including grid-connected, islanded, and transitional modes. Results demonstrate high forecasting accuracy, effective interpretation of system states, optimized DER operation, and seamless communication within the MIL environment.**

***Index Terms*—Forecasting, microgrid, model-in-the-loop, optimization, tertiary control layer**

I. Introduction

Microgrids comprising distributed energy resources (DERs) such as photovoltaic (PV) systems, wind farms, energy storage systems (ESS), and diesel generators (DiG), these networks are no longer passive entities but active participants in grid management. Microgrids are capable of enhancing flexibility, reliability, and sustainability across modern power systems. To coordinate their diverse assets and ensure stable and economical operation, hierarchical control architectures, consisting of primary, secondary, and tertiary control layers have become standard for microgrid operation [1]. While the primary and secondary layers focus on local voltage and frequency regulation, the tertiary control layer operates at the system-level, optimizing power dispatch, cost, and energy exchange with the main grid. It is responsible for economic dispatch, peak-load management, reactive power compensation, and resilience enhancement by considering both current and forecasted operating conditions [2].

Microgrids have two distinct operational modes: grid-connected mode (GCM) and islanded mode (ISM), and tertiary control layer of a microgrid needs to consider the operational modes, and all possible transition scenarios such as Grid to Island (G2I), and Island to Grid (I2G) in its embedded algorithm. Different types of optimization techniques including linear programming (LP), mixed integer based programming (MIP), heuristic and metaheuristic methods, machine learning based methods such as reinforcement learning have been applied to solve complex operational and planning problems in microgrids [3]. However, most existing studies evaluate these tertiary control strategies in simulation-only environments where model assumptions are idealized and do not reflect the stochastic, nonlinear dynamics of real microgrids [4]. Moreover, there remains a lack of comprehensive frameworks demonstrating how a tertiary control layer can be physically integrated and validated within a real or emulated microgrid through model-in-the-loop (MIL) or hardware-in-the-loop (HIL) environments. Such validation is essential to assess the control layer's robustness under real-time environments, dynamic behavior and transitions of a microgrid. Critically, validating the performance in a low-risk MIL/HIL environment is also more economical and safer prior to field deployment.

Forecasting is another important element in tertiary control in order to perform optimization for microgrids considering future time horizon. Accurate forecasting improves the performance of the tertiary control algorithm for the operation, control, and planning of DERs, leading to improved efficiency, reliability, and cost savings [5]. Recent advancements in machine learning (ML) have improved forecasting accuracy for renewable generation and load demand [6], particularly with models such as long short-term memory (LSTM) networks, Neural Prophet (NP), and transformer model.

This paper proposes a framework to integrate the tertiary control layer of Center for Microgrid Research (CMR) Microgrid in a MIL environment to validate its performance in different dynamic scenarios. The virtual model reflects the real-world CMR Microgrid system which consists of both primary and secondary control layer. The virtual model is validated extensively with real field data of the CMR Microgrid to reflect real-world system behavior. The paper also proposes a LSTM based load and PV forecasting model and the integration procedure of the forecasting model in the tertiary control layer. The major contributions of this work are:

- Integrating the tertiary control layer with the virtual CMR

979-8-3315-8138-1

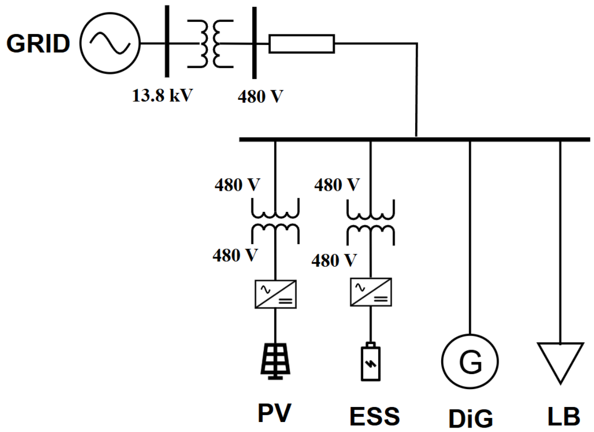

Fig. 1. One line diagram of CMR Microgrid.

Microgrid model in Typhoon HIL environment

- Integration of LSTM based load and PV forecasting model with the tertiary control algorithm based on real-world CMR Microgrid data
- Validating the effectiveness of the proposed tertiary control layer framework with CMR Microgrid's dynamic operating scenarios

II. CMR Microgrid's System Description

The CMR Microgrid is a 60 Hz 480Vac 3 Phase 4 wire electrical system. The CMR Microgrid includes the utility grid, DiG, ESS, PV system, and Loadbank (LB). The one-line diagram of the CMR Microgrid is presented in Fig. 1. The DiG has active power rating of 50 kW in grid-following mode with 62 kVA ratings and minimum 0.85 power factor. The ESS has a capacity of 394 kWh at 125 kW which is connected to a bi-directional 125 kVA inverter. The solar PV array is rated for 48-kWdc, connected to a 125 kVA inverter and the LB has a capacity of 240 kW and 186 kVAR. A digital model of CMR Microgrid is developed on a digital real-time simulator using data driven approach to replicate the real world performance of the CMR Microgrid.

III. Objectives of Tertiary Control Algorithm

This section outlines the primary objectives that define the functionality of the tertiary control layer in the CMR Microgrid. The problem of tertiary control layer is divided into two subcategories in this paper: forecasting, and optimization.

A. Load and PV Forecasting

Two important forecasting categories for the CMR Microgrid control system are load forecasting and PV generation forecasting. In order to perform cost optimization, predicted load and PV values are required so that future steps can be considered into the tertiary optimization algorithm. To accurately train any forecasting model, real-world data is a must. The real-world CMR Microgrid building load data is collected with 1 minute resolution from February 2023 till August 2024 and the PV system output data is collected from February 2022 till December 2023. These datasets are preprocessed for any missing and inaccurate datasets and then resampled at 5 minute resolution.

To address the forecasting component of the tertiary control layer, LSTM network is implemented for both load and PV forecasting. LSTM is a specialized deep learning architecture designed to overcome the short-term dependency limitations of traditional recurrent neural networks by effectively capturing long-term temporal dependencies in time-series data [7]. Its ability to model complex nonlinear relationships makes it particularly suitable for predicting patterns in load demand and solar PV generation. The LSTM architecture consists of four key components: the forget gate, input gate, memory cell, and output gate. These components work together to regulate the flow of information through the network over time. The mathematical representation of the LSTM model implemented in this work is based on [8]. The objective of the forecasting model is to minimize the error between the actual and forecasted values which is formulated using mean absolute error method provided in (1) where $\hat{F_v}$ is forecasted value, A_v is actual value, t is time period, and T is prediction horizon.

$$\min\left\{\frac{1}{T}\sum_{t=1}^{T}\left|A_v(t)-\hat{F_v}(t)\right|\right\} \tag{1}$$

B. Optimization

The current tertiary control layer performs optimization for determining the optimal peak load to reduce the demand charge cost from the grid and optimum operational setpoints of individual DERs to minimize the overall operational cost of the CMR Microgrid.

1) Optimal Peak Determination: The objective is to determine the optimum peak in GCM while ensuring resiliency to the CMR Microgrid for sudden power outage. As a result, the problem is designed with two objectives; one is to reduce peak demand cost and the other is to utilize minimum power from microgrid resources. Therefore, the objective function for this problem can be expressed by (2) where C_{DiG} is cost of using DG, C_{ESS} is cost of using ESS, C_{Grid} is grid power usage cost, C_{Re} is resiliency cost, and ω is the weight factor. Solution to this problem will determine the maximum power the microgrid should absorb from the grid. The output of this algorithm is one of the input for the cost minimization problem. Differential Evolution (DE) [9] was used to determine the optimal peak based on CMR Microgrid's historical load consumption pattern.

$$min\left\{\sum_{t=1}^{t=T}(\omega\times(C_{DiG}\left(t\right)+C_{ESS}\left(t\right)+C_{Grid}(t))+ (1-\omega)\times C_{Re}(t)\right\} \tag{2}$$

2) Operational Cost Minimization: One of the main goal of the tertiary control layer is to minimize overall operating costs of CMR Microgrid by strategically deploying its resources. In

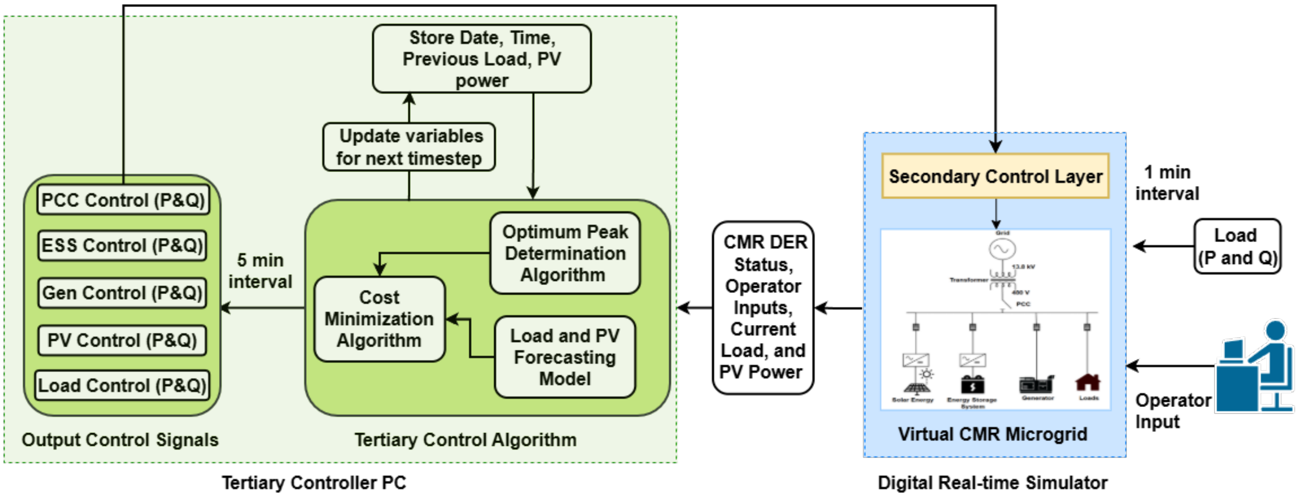

Fig. 2. Integration of tertiary control layer with virtual CMR Microgrid model.

GCM, the main objective is to reduce the total operational cost of the microgrid utilizing all the available resources. In ISM, when the demand is higher than the generation, the objective is to perform load shedding based on the importance of the load to ensure stability of the system. The objective function of cost optimization problem is expressed by (3) where C_{PV} is cost of using PV and C_{LS} is cost of shedding load.

$$min\left\{\sum_{t=1}^{t=T}(C_{DiG}(t)+C_{ESS}(t)+C_{Grid}(t)+ C_{PV}(t)+C_{LS}(t)\right\} \quad (3)$$

These objective functions are subject to different types of constraints that include active and reactive power balance, power limits of the resources, power factor limits, apparent power limits, DiG fuel limit, and ESS state of charge (SOC) limit. Mixed Integer Non-Linear Programming (MINLP) [10] was used to solve the cost minimization problem of the CMR Microgrid, implemented using python-Gurobi API.

IV. Integration of Tertiary Control Layer with Virtual CMR Microgrid Model

This section describes the integration of the tertiary control layer with the virtual CMR Microgrid model and the test setup for validating its performance. The integration of the tertiary control layer to the virtual CMR Microgrid model is an essential step to enable two-way communication that reflects real-world operational environments. The integration allows for coordinated operation across all three control layers and provides a realistic platform for performance validation of tertiary control algorithms in MIL environment. The integration framework also enables real-time interaction between the control algorithm and the virtual CMR Microgrid.

Figure 2 illustrates the architecture for integrating the tertiary control algorithm with CMR Microgrid model. The virtual CMR Microgrid is developed in digital real-time simulator and validated using real-world field data. The model is simulated in real-time and CMR Microgrid's load data is fed to the model at 1 minute interval. Tertiary control layer is running at 5 minute interval in a computer. The tertiary control layer receives the operator inputs, load and PV power and system status from the model. Based on load and PV power, it generates the forecasted values for load and PV. The optimum peak determination algorithm generates the optimum peak value based on the time and date and historical pattern of that month. Forecasted values and optimal peak load are then sent to the cost minimization algorithm. Based on these and other inputs from the model, the tertiary control provides P and Q reference values for all DERs. The tertiary control layer then update the file that stores load, PV power, time, ESS estimated SOC so that these variables are upto date for the next timestep. The control output signals for each DERs are then sent to the secondary control layer of the CMR Microgrid's virtual model which operates its control loops based on the setpoints provided by tertiary control. This closed-loop system with tertiary control layer enables dynamically optimize the operations through real-time forecasting and control signal updates.

V. Results and Validation

This section evaluates the performance of the tertiary control layer with forecasting model and its integration framework through forecasting accuracy analysis and various case studies to demonstrate the effective application of the tertiary control layer in MIL environment. The data from the virtual model is captured at 5 minutes interval for the analysis of the results.

A. Forecasting

To test the forecasting model, the preprocessed real-world CMR Microgrid data set is split into training, validation, and testing as a ratio of 70:15:15. Model performance is evaluated

979-8-3315-8138-1

using two statistical metrics: mean absolute error (MAE) and mean absolute percentage error (MAPE).

$$MAE = \frac{1}{N}\sum_{i=1}^{N} |\widehat{p_i} - p_i| \tag{4}$$

$$MAPE = \frac{1}{N}\sum_{i=1}^{N} \left|\frac{\widehat{p_i} - p_i}{p_i}\right| \times 100 \tag{5}$$

Where N is number of data points, $\widehat{p_i}$ is predicted value, p_i is actual value. To calculate the MAPE for PV forecasting, the denominator p_i is changed to PV rated capacity which is based on [11]. The LSTM based forecasting model is also compared with another ML based model, NP and the hyperparameters such as learning rate, batch size, number of past observations, and random seed for both models are kept constant. Table I presents the comparison of the forecasting performance of the two models. For load forecasting, both models perform very closely. However, LSTM performance is 0.5% better than NP for PV forecasting. This improvement, though seemingly modest, is significant in the context of renewable energy forecasting. Given that accurate forecasting directly impacts the optimization performance of the tertiary control layer, LSTM is used as the forecasting model in the tertiary control layer for its more accurate results.

B. GCM Operation

In this case, all CMR Microgrid resources are available for operation. Initially, the algorithm sends signal to use the full amount of PV and to use grid power for rest of the load which can be seen in Fig. 3. An optimal peak for the specific month is determined to be 88 kW by the algorithm. During peak period when the load is higher than 88 kW, the algorithm sends signal to dispatch ESS for providing additional power to keep power contribution from the grid around 88 kW but no DiG dispatch signals are sent due to its higher cost. The framework is able to reflect the desired system behavior in the model by accurately sending the output control signals to the model.

In this case, it is assumed there is no ESS. To achieve that, operator can select to disable ESS in real-time from the runtime panel of the virtual model. From Fig. 3, it can be seen that the algorithm sends signal to turn on the DiG in order to maintain grid power around 88 kW as it considers there is no ESS in the system.

TABLE I
COMPARISON OF FORECASTING RESULT

Performance Metrics	Data	Load Forecasting		PV Forecasting	
		LSTM	NP	LSTM	NP
MAE (kW)	Training	2.90	2.92	0.70	0.94
	Validation	2.04	1.96	0.60	0.70
	Testing	1.41	1.40	0.53	0.72
MAPE (%)	Training	6.60	6.62	1.54	2.10
	Validation	5.34	5.42	1.24	1.52
	Testing	4.60	4.52	1.18	1.60
Training Time (s)		300	60	77.5	21

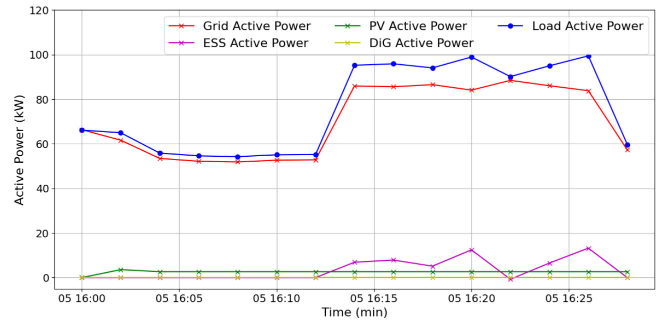

Fig. 3. Active power profile during GCM operation when all resources are available.

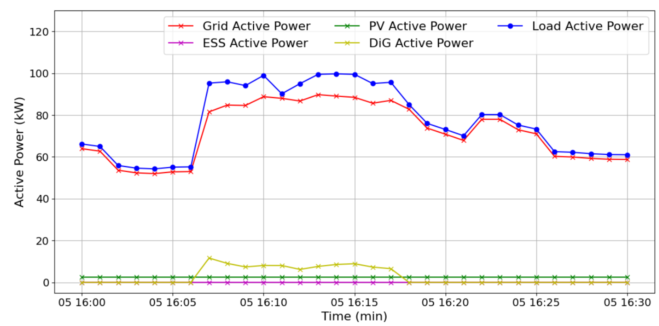

Fig. 4. Active power profile during GCM operation with no ESS.

C. ISM Operation

During ISM operation the tertiary control layer generates active power reference signals for ESS and DiG and sends to the secondary control layer which sends appropriate control signals to the DERs to reflect the tertiary control outputs. Fig. 5 shows how the load is shared between the ESS and DiG during ISM operation. The tertiary control algorithm prioritizes the ESS for supplying the majority of the load demand, while minimizing or avoiding the use of the DiG whenever possible due to its higher operational cost.

D. G2I and I2G Transitions

This study is conducted to evaluate the effectiveness of the tertiary control layer during the CMR Microgrid's transition from G2I and I2G. As tertiary control will operate based on

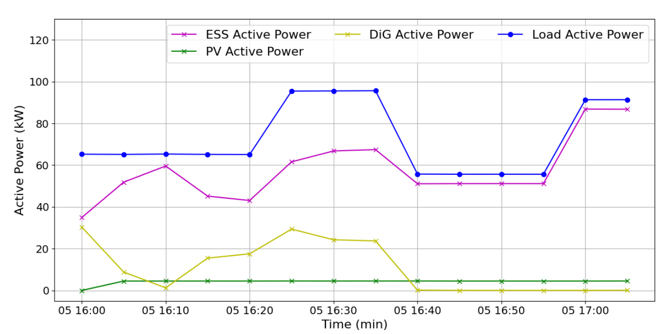

Fig. 5. Active power profile during ISM operation.

979-8-3315-8138-1

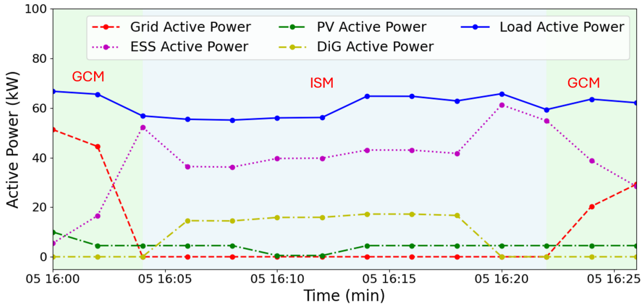

Fig. 6. Active power profile during GCM and ISM operations with transitions.

economic factors in GCM, the grid power is limited to 40 kW to demonstrate the algorithm's performance. The active power profile for this case is shown in Fig. 6. At time, t = 16:04, the system transitions to ISM based on the operator's islanding command from the model's runtime panel. Based on islanding command, the tertiary controller sends control signals to decrease the grid power to zero, and ramp up ESS output to maintain demand. Subsequently, the DiG is activated in ISM to share the load with the ESS as required. At time, t = 16:22, the system returns to GCM based on the operator command, and the tertiary sends signals to resume grid active power alongside the local resources.

E. Load Shedding in ISM

This study is conducted to evaluate the effectiveness of the tertiary control layer under ISM with load shedding scenario which is represented in Fig. 7. To demonstrate this case, ESS is assumed to have only 5% of its available SOC. So, during ISM operation, DiG is supplying most of the load due to low ESS SOC. When ESS reaches its minimum SOC threshold and the tertiary control algorithm sends command to initiate controlled load shedding of flexible load as total demand becomes higher than the current generation capability.

VI. Conclusion

The developed MIL framework successfully demonstrates the integration of a forecast-driven tertiary control layer with the virtual CMR Microgrid model, enabling real-time validation of system-level optimization and transition performance under realistic conditions. The LSTM-based forecasting model provides accurate load (around 94%) and PV (around 98.5%) predictions, outperforming the NP by 0.5% which enables the tertiary algorithm to accurately consider load and PV for future time-steps. The results from several case studies confirm the framework's capability to perform under different operational modes with operator inputs, transitions between the modes, and load shedding scenarios in ISM for the CMR Microgrid system. The average execution time of the proposed tertiary control algorithm is approximately 3.2s per control cycle when executed on a standard local computer. This runtime is well within the operational timescale of tertiary control, confirming the feasibility of real-time deployment within the proposed framework. The MIL-based validation provides an economical and low-risk platform for assessing tertiary control performance prior to field deployment, ensuring robustness against dynamic operational scenarios and establishing the foundation for future CHIL and real-world integration.

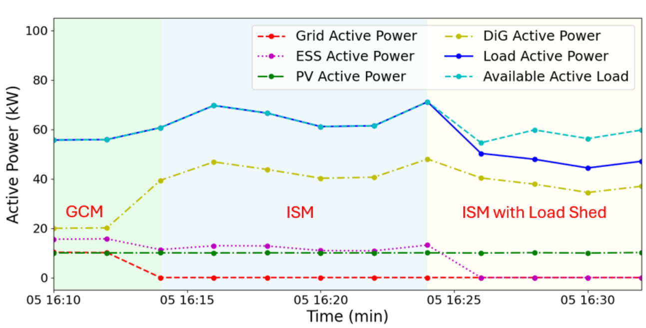

Fig. 7. Active power profile during ISM operation with load shedding.

Acknowledgment

This effort is sponsored by the U.S. Government under other transaction for prototype agreement number W9132T239C007 between University of St. Thomas and the Government. The U.S. Government is authorized to reproduce and distribute reprints for Governmental purposes notwithstanding any copyright notation thereon.

References

[1] J. Gutiérrez-Escalona, C. Roncero-Clemente, O. Husev, O. Matiushkin, and F. Blaabjerg, "Artificial intelligence in the hierarchical control of ac, dc and hybrid ac/dc microgrids–a review," *IEEE Access*, 2024.

[2] F. Nawaz, E. Pashajavid, Y. Fan, and M. Batool, "A comprehensive review of the state-of-the-art of secondary control strategies for microgrids," *IEEE Access*, vol. 11, pp. 102 444–102 459, 2023.

[3] S. A. Juma, S. P. Ayeng'o, and C. Z. Kimambo, "A review of control strategies for optimized microgrid operations," *IET Renewable Power Generation*, vol. 18, no. 14, pp. 2785–2818, 2024.

[4] S. Ahmad, M. Shafiullah, C. B. Ahmed, and M. Alowaifeer, "A review of microgrid energy management and control strategies," *IEEE Access*, vol. 11, pp. 21 729–21 757, 2023.

[5] G. Manzolini, A. Fusco, D. Gioffrè, S. Matrone, R. Ramaschi, M. Saleptsis, R. Simonetti, F. Sobic, M. J. Wood, E. Ogliari *et al.*, "Impact of pv and ev forecasting in the operation of a microgrid," *Forecasting*, vol. 6, no. 3, pp. 591–615, 2024.

[6] M. J. A. Shohan, M. O. Faruque, and S. Y. Foo, "Forecasting of electric load using a hybrid lstm-neural prophet model," *Energies*, vol. 15, no. 6, p. 2158, 2022.

[7] S. Hochreiter and J. Schmidhuber, "Long short-term memory," *Neural computation*, vol. 9, no. 8, pp. 1735–1780, 1997.

[8] A. K. Dubey, A. Kumar, V. García-Díaz, A. K. Sharma, and K. Kanhaiya, "Study and analysis of sarima and lstm in forecasting time series data," *Sustainable Energy Technologies and Assessments*, vol. 47, p. 101474, 2021.

[9] P. Tiwari, V. N. Mishra, and R. P. Parouha, "Developments and design of differential evolution algorithm for non-linear/non-convex engineering optimization," *Archives of Computational Methods in Engineering*, vol. 31, no. 4, pp. 2227–2263, 2024.

[10] J. Kronqvist, D. E. Bernal, A. Lundell, and I. E. Grossmann, "A review and comparison of solvers for convex minlp," *Optimization and Engineering*, vol. 20, no. 2, pp. 397–455, 2019.

[11] J. Zhang, B.-M. Hodge, A. Florita, S. Lu, H. F. Hamann, and V. Banunarayanan, "Metrics for evaluating the accuracy of solar power forecasting," National Renewable Energy Lab.(NREL), Golden, CO (United States), Tech. Rep., 2013.